Structural Coupling between the Oxygen-Evolving Mn Cluster and a Tyrosine Residue in Photosystem II As Revealed by Fourier Transform Infrared Spectroscopy†

Takumi Noguchi,*,‡ Yorinao Inoue,‡ and Xiao-Song Tang*,§

Photosynthesis Research Laboratory, The Institute of Physical and Chemical Research (RIKEN), Wako, Saitama 351-01, Japan, and E. I. du Pont de Nemours & Company, Central Research and Development Department, Wilmington, Delaware 19880-0173

Received July 18, 1997; Revised Manuscript Received October 2, 1997⊗

ABSTRACT: The flash-induced Fourier transform infrared (FTIR) difference spectrum of the oxygen-evolving Mn cluster upon S_1-to-S_2 transition (S_2/S_1 spectrum) was measured using photosystem II (PS II) core complexes of *Synechocystis* 6803 in which tyrosine residues were specifically labeled with ^{13}C at the ring-4 position. The double-difference spectrum between the unlabeled and labeled S_2/S_1 spectra showed that the bands at 1254 and 1521 cm^{-1} downshifted by 25 and 15 cm^{-1}, respectively, upon ring-4-^{13}C-Tyr labeling. This observation indicates that there is a tyrosine residue coupled to the Mn cluster, and the vibrational modes of this tyrosine are affected upon S_2 formation. From a comparison of the above band positions and isotopic shifts in the S_2/S_1 spectrum with those of the FTIR spectra of tyrosine in aqueous solution at pH 0.6 (Tyr-OH) and pH 13.4 (Tyr-O^-) and of the $Y_D^{\bullet}/Y_D$ FTIR difference spectrum, the 1254 and 1521 cm^{-1} bands were assigned to the CO stretching and ring CC stretching modes of tyrosine, respectively, and this tyrosine was suggested to be protonated in PS II. The observation that the effect of the S_2 formation on the tyrosine bands appeared as a decrease in intensity with little frequency change could not be explained by a simple electrostatic effect by Mn oxidation, suggesting that the Mn cluster and a tyrosine are linked via chemical and/or hydrogen bonds and the structural changes of the Mn cluster are transmitted to the tyrosine through these bonds. On the basis of previous EPR studies that showed close proximity of Y_Z to the Mn cluster, Y_Z was proposed as the most probable candidate for the above tyrosine. This is the first demonstration of the structural coupling between Y_Z and the Mn cluster in an intact oxygen-evolving complex. This structural coupling may facilitate electron transfer from the Mn cluster to Y_Z. Our observation also provides an experimental support in favor of the proton or hydrogen atom abstraction model for the Y_Z function.

Photosystem II (PS II)[1] in cyanobacteria and plants utilizes light energy to convey an electron across the thylakoid membrane from the lumenal side to the stromal side. Charge separation takes place in the singlet excited state of P680, and pheophytin is first reduced as the primary electron acceptor; the electron is further transferred to Q_A and then to Q_B. On the electron donor side, a hole moves from $P680^+$ to the oxygen-evolving complex (OEC) through the redox-active tyrosine Y_Z (tyrosine-161 of the D1 polypeptide). In OEC, two water molecules are oxidized as the terminal electron donor to be cleaved into molecular oxygen and protons. Another redox-active tyrosine, Y_D (tyrosine-160 of the D2 polypeptide), which is symmetrically positioned with respect to Y_Z, is an auxiliary electron donor to $P680^+$ but does not work in the functional electron transfer pathway (reviewed in ref 1).

Oxygen-evolving reactions in OEC proceed through the so-called S-state cycle that comprises five intermediate states, S_i ($i = 0-4$) (*2*, *3*). Each S state except S_4 is advanced to the next state by single-flash illumination. Molecular oxygen evolves upon S_3-to-S_0 transition through the unstable S_4 state. The S_1 state is thermally stable, and hence dark-adapted PS II requires three flashes to evolve first oxygen, and afterward period-four oscillation of oxygen evolution is observed. OEC is thought to consist of four Mn ions with Ca^{2+} and Cl^- as indispensable cofactors. The structure of OEC has been investigated mainly by EPR and EXAFS studies (reviewed in refs 4 and 5). The core structure of the OEC is considered to be a tetranuclear Mn cluster modeled as a dimer of dimers, in which two di-μ-oxo bridged dimers are linked by a μ-oxo bridge (*6*). Site-directed mutagenesis studies have provided candidates of amino acid ligands of the Mn cluster, and they are mainly located on the D1 polypeptide (reviewed in ref 4). However, the exact location of the OEC is yet to be clarified.

Recently, it has been proposed that $Y_Z^{\bullet}$ functions not only as an immediate oxidant of the Mn cluster but also as a direct abstractor of protons or hydrogen atoms from substrate water (*5*, *7*−*10*). This idea (*7*−*9*) came from the following

† This research was supported by a grant for Photosynthetic Sciences and Biodesign Research Program at The Institute of Physical and Chemical Research (RIKEN) given by the Science and Technology Agency (STA) of Japan and was partially supported by the Central R&D Department of E. I. du Pont de Nemours & Co. (Contribution 7661).

* Authors to whom correspondence should be addressed.

‡ RIKEN.

§ du Pont de Nemours & Co.

⊗ Abstract published in *Advance ACS Abstracts,* November 15, 1997.

[1] Abbreviations: EPR, electron paramagnetic resonance; EXAFS, extended X-ray absorption fine structure; FTIR, Fourier transform infrared; Mes, 2-(*N*-morpholino)ethansulfonic acid; IR, infrared; OEC, oxygen-evolving complex; P680; primary electron donor of PS II; PS II, photosystem II; Q_A, primary quinone electron acceptor of PS II; Q_B, secondary quinone electron acceptor of PS II; XANES, X-ray absorption near edge structure; Y_D, redox-active tyrosine 160 of the D2 polypeptide; Y_Z, redox-active tyrosine 161 of the D1 polypeptide.

S0006-2960(97)01760-1 CCC: $14.00

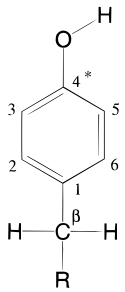

FIGURE 1: Numbering of tyrosine side chain. The carbon at the ring-4 position (marked by *) was labeled with ^{13}C.

observations: (1) the motional flexibility of $Y_Z^\bullet$ (*8, 9, 11*); (2) the lack of a well-ordered hydrogen bond for $Y_Z^\bullet$ (*12*−*14*); and (3) the estimation of the short distance between the Mn cluster and Y_Z (4.5 Å) based on the assignment of the "split S_3 signal" in Ca^{2+}-depleted PS II to $Y_Z^\bullet$ (*9, 10*). The distance between the Mn cluster and Y_Z, however, has been estimated as >10 Å from the lack of broadening of the $Y_Z^\bullet$ EPR signal by the presence of the Mn cluster (*15*) or as 15−20 Å from the measurement of relaxation enhancement of $Y_Z^\bullet$ due to the dipole interaction with the Mn cluster (*16*). Also, very recently, Astashkin et al. (*17*) have reported another interpretation of the split S_3 signal—that this signal originates from the coupling between $Y_Z^\bullet$ and another organic radical with a distance of 5.3 Å. Furthermore, none of the experiments studying the flexibility and the hydrogen-bonding state of $Y_Z^\bullet$ have been carried out with O_2-evolving PS II samples (*7, 8, 11*−*14*). Thus, the idea of direct involvement of $Y_Z^\bullet$ in the oxygen-evolving reaction is still controversial.

Light-induced FTIR difference spectroscopy has been used to investigate the structures and microenvironments of cofactors and their interactions with the surrounding molecules in photosynthetic proteins (for reviews, see refs 18 and 19). As for the Mn cluster in PS II, flash-induced FTIR difference spectra between S_1 and S_2 states (S_2/S_1) have been obtained and the presence of carboxylate ligands of the Mn cluster and the protein conformational changes upon S_2 formation have been reported (*20*−*25*). Comparison of the S_2/S_1 spectrum of normal PS II with that of Ca^{2+}-depleted PS II has shown that Mn and Ca^{2+} are connected by a carboxylate bridge and that this coordination structure drastically changes upon S_2 formation (*23*). Furthermore, an H_2O/D_2O exchange experiment has shown that there is another carboxylate ligand that forms a strong hydrogen bond with a substrate water molecule (*24*).

In this study, structural coupling between the Mn cluster and Y_Z was investigated by FTIR difference spectroscopy. An S_2/S_1 difference spectrum of the Mn cluster was measured using the PS II core complexes isolated from *Synechocystis* 6803 in which tyrosine side chains were labeled with ^{13}C at the ring-4 position (ring-4-^{13}C-Tyr) (Figure 1). This labeling enabled us to identify tyrosine bands in the S_2/S_1 spectrum. To analyze the data, we also measured a $Y_D^\bullet/Y_D$ difference spectrum and spectra of tyrosine in aqueous solutions and examined the isotopic effect on these spectra. The role of the coupling between the Mn cluster and Y_Z is discussed with respect to the electron transfer reaction as well as the putative Y_Z function of proton or hydrogen atom abstraction from substrate water.

MATERIALS AND METHODS

Cells of wild-type *Synechocystis* 6803 strain were grown photoautotrophically in BG-11 medium (*26*) at 30 °C for 5 days in 10-L carboys using cool-white fluorescent lamps (7 W/m^2). The growth medium was bubbled with 5% CO_2 in air. For isotopic labeling experiments, cells were grown photoautotrophically in BG-11 medium containing 0.5 mM phenylalanine, 0.25 mM tryptophan, and 0.25 mM ring-4-^{13}C-labeled tyrosine for 6−7 days following the method of Barry and Babcock (*27*). Oxygen-evolving PS II core complexes from *Synechocystis* were purified according to the procedure described earlier (*28*) and suspended in 50 mM Mes−NaOH (pH 6.0) buffer containing 20% (w/v) glycerol, 5 mM $MgCl_2$, 5 mM $CaCl_2$, and 0.03% dodecyl maltoside. Oxygen-evolving PS II membranes from spinach (*29*) were prepared according to the procedure of Ono and Inoue (*30*).

For the FTIR measurements of S_2/S_1 spectra, the PS II core complexes of *Synechocystis* were resuspended in 5 mM Mes−NaOH (pH. 6.0) buffer containing 50 mM sucrose, 5 mM NaCl, and 5 mM $CaCl_2$, and then this suspension was concentrated to about 6 mg of Chl/mL using a Microcon 100 (Amicon). After 5 μL of the core suspension was mixed with 4 μL of ferricyanide/ferrocyanide (2 mM/18 mM) solution, the sample was lightly dried on a BaF_2 plate under N_2 gas flow passed through water and then covered with another BaF_2 plate. The sample of spinach PS II membranes for the S_2/S_1 measurement was prepared as described previously (*23, 24*). For $Y_D^\bullet/Y_D$ measurement, the PS II core complexes of *Synechocystis* were treated with 10 mM NH_2-OH to deplete the Mn cluster, and then the suspension was washed with 4 mM Mes−NaOH buffer (pH 6.0) containing 40 mM sucrose and 2 mM NaCl using a Microcon-100. The Mn-depleted PS II core complexes (~0.6 mg of Chl/mL, 50 μL) were then treated with 100 mM sodium formate and incubated on ice for 1 h. This formate treatment increases the midpoint potential of the non-heme iron (*31*) and prevents its preoxidation at even a relatively high redox potential of buffer in the presence of ferricyanide (*32*). After the PS II suspension was concentrated to 5 μL volume, 3 μL of ferricyanide/ferrocyanide (19 mM/1 mM) solution was mixed into the sample. The mixture was then lightly dried on a BaF_2 plate under N_2 gas and covered with another BaF_2 plate.

FTIR measurements were performed as described previously (*23, 24*). Briefly, spectra were measured on a JEOL JIR-6500 spectrophotometer equipped with an MCT detector (EG&G Judson IR-DET101) and the sample temperature was adjusted to 250 K in a liquid N_2 cryostat (Oxford DN1704). Difference spectra were obtained by subtraction between the two single-beam spectra (150 s accumulation for each) measured before and after flash illumination. A frequency-doubled Nd:YAG laser (Quanta-Ray GCR-130) (532 nm; 7 ns pulse width) was used for illumination, and for the S_2/S_1 spectra a single pulse was introduced to the sample at a saturating intensity of 20 mJ/(pulse cm^2). For the $Y_D^\bullet/Y_D$ spectra, two pulses at a 1 s interval were introduced. The reason for using only two pulses is to prevent the contamination of heat bands in the spectra. Spectral resolution was 4 cm^{-1}. Three to five spectra were averaged for the S_2/S_1 spectra, and two spectra were averaged for the $Y_D^\bullet/Y_D$ spectra. One sample was repeatedly used to obtain a maximum of three spectra by incubating the sample at 278 K for at least 10 min after each measurement. It was

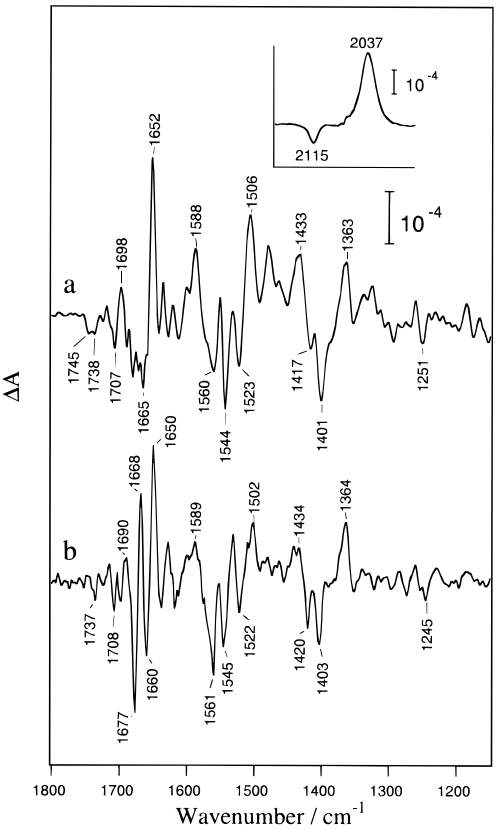

FIGURE 2: Flash-induced FTIR difference spectra of the OEC upon S_1-to-S_2 transition (S_2/S_1 difference) measured using PS II core complexes of *Synechocystis* 6803 (a) and PS II membranes of spinach (b). A ferricyanide/ferrocyanide (2 mM/18 mM) mixture was present in the samples to obtain the S_2/S_1 spectra free from acceptor-side signals. (Inset) CN stretching region of the *Synechocystis* S_2/S_1 spectrum, showing that ferricyanide indeed abstracts an electron from the protein. Flash illumination was performed by a single pulse from a Nd:YAG laser (532 nm, 7 ns). Sample temperature was 250 K.

ascertained that an identical spectrum was obtained each time. No smoothing procedure was applied to the spectra.

FTIR spectra of unlabeled and ring-4-^{13}C-labeled L-tyrosine in aqueous solutions were measured using a TGS detector at room temperature. Tyrosine (2% w/v) was dissolved in 0.5 M HCl solution (final pH was 0.6) as a protonated state (designated Tyr-OH) or in 0.5 M NaOH solution (final pH was 13.4) as a deprotonated state (Tyr-O^-). The sample solution was placed between ZnSe plates with a ~7 μm spacer. The spectra of the HCl and NaOH solutions in the absence of tyrosine were measured and subtracted from the spectra of Tyr-OH and Tyr-O^-, respectively, so as to cancel the H_2O band around 1643 cm^{-1}.

RESULTS

In Figure 2a is shown a flash-induced FTIR difference spectrum of OEC upon S_1-to-S_2 transition measured using the PS II core complexes of *Synechocystis* 6803. The method of measuring the S_2/S_1 spectrum of the core complexes free from acceptor-side signals followed that previously used for the PS II membranes (*23*, *24*, *35*). The presence of the ferricyanide/ferrocyanide (2 mM/18 mM) mixture and the relatively low pH (pH 6.0) keep the non-heme iron in the reduced state of Fe^{2+} (*35*), and simultaneously ferricyanide works as an exogenous electron acceptor. A negative band at 2115 cm^{-1} and a positive band at 2037 cm^{-1} (inset) arising from the CN modes of ferricyanide and ferrocyanide, respectively, show that ferricyanide indeed abstracted an electron from the protein. The S_2/S_1 spectrum of PS II membranes of spinach is presented in Figure 2b for comparison. Most of the spectral features are conserved in the two spectra; bands in the region of the symmetric stretch of carboxylate (1363, 1401, 1417, and 1433 cm^{-1} in *Synechocystis* vs 1364, 1403, 1420, and 1434 cm^{-1} in spinach) and those in the region of the asymmetric stretch of carboxylate and of the amide II mode of protein backbone (1506, 1523, 1544, 1560, and 1588 cm^{-1} in *Synechocystis* vs 1502, 1522, 1545, 1561, and 1589 cm^{-1} in spinach) are observed practically in the same positions. In the amide I region (1600−1700 cm^{-1}), however, the spectral features are rather different. The spectrum of *Synechocystis* shows a relatively simple structure with a strong positive band at 1652 cm^{-1} and a negative band at ~1665 cm^{-1} (Figure 2a), while a complex band feature is seen in the spectrum of spinach (Figure 2b). The spectral changes in the amide I region imply perturbation of the secondary structures of proteins upon S_2 formation (*23*, *24*). It has been reported that the amide I bands in the S_2/S_1 spectrum are sensitive to the cryoprotectant species and temperature (*21*), indicating that the protein movement in the OEC is influenced by the environment and condition of the PS II protein. The observed disagreement in the amide I bands between *Synechocystis* and spinach, therefore, may be due to not only the difference in species (cyanobacterium vs higher plant) but also the differences in preparation (core complexes vs membranes) and subtle sample condition for the measurement. It is noted that the positive bands at 1479 and ~1330 cm^{-1} in the S_2/S_1 spectrum of *Synechocystis* (Figure 2a), which are not observed in the spectrum of spinach (Figure 2b), may represent small contaminations of Q_A^-/Q_A (*32*, *33*) and Fe^{2+}/Fe^{3+} (*34*, *35*) signals, respectively. However, the contribution of these contaminating acceptor-side signals to the *Synechocystis* S_2/S_1 spectrum must be very small judging from the above-mentioned consistency of the main bands with those in the spinach S_2/S_1 spectrum except in the amide I region. The plausible explanation for the small contamination of acceptor-side signals is that in the core complexes of *Synechocystis*, an electron is less easily abstracted by ferricyanide compared with the membranes of spinach due to some changes on the electron-acceptor side such as the absence of Q_B and the possible shift of the midpoint potential of the non-heme iron.

Recently, Steenhuis and Barry (*36*) reported $S_2Q_A^-/S_1Q_A$ FTIR difference spectra (1600−1770 cm^{-1} region) measured with PS II preparations of plant and *Synechocystis* using continuous light illumination at 200 K, but their spectra were considerably different from our S_2/S_1 spectra (Figure 2; *23*, *24*). This inconsistency is reasonable because the Q_A^-/Q_A signals have large contribution in the $S_2Q_A^-/S_1Q_A$ spectrum and thus the S_2/S_1 signals are actually buried under the Q_A^-/Q_A signals [refer to the spectral scales of the S_2/S_1 (*20*, *23*−*25*, *35*) and Q_A^-/Q_A (*20*, *32*, *33*) spectra measured using similar BBY-type PS II membranes and also compare these spectra with the $S_2Q_A^-/S_1Q_A$ spectrum by Noguchi et al. (*20*, *22*)] .

Figure 3 shows an S_2/S_1 spectrum of ring-4-^{13}C-Tyr-labeled core complexes of *Synechocystis* (b) compared with a spectrum of unlabeled core complexes (a). While almost all of the major bands are conserved between the two spectra, it is evident that a negative peak at 1251 cm^{-1} downshifts

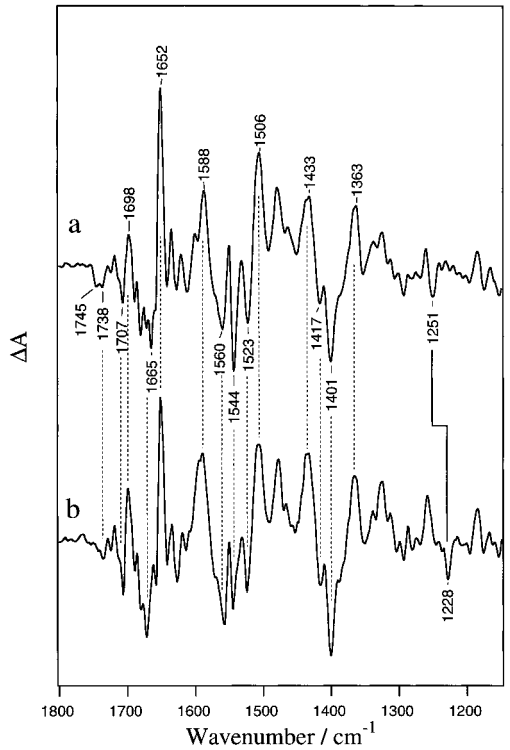

FIGURE 3: S_2/S_1 difference spectrum of ring-4-^{13}C-Tyr-labeled PS II core complexes of *Synechocystis* 6803 (b) compared with the spectrum of unlabeled core complexes (a). Measurement conditions were the same as for Figure 2.

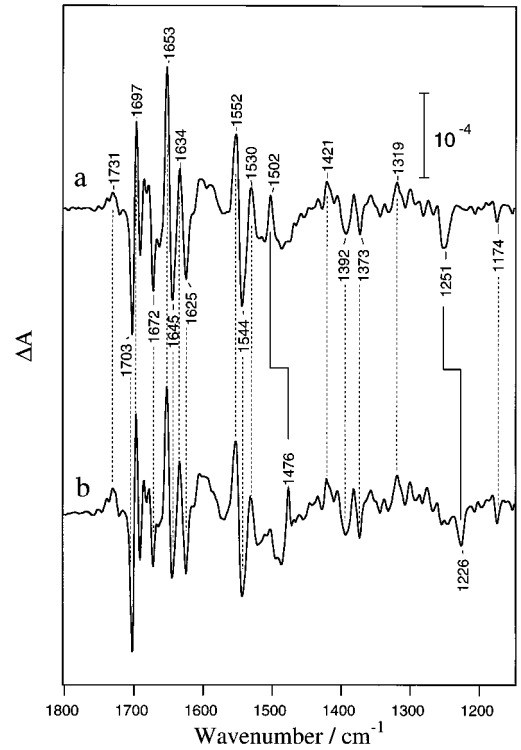

FIGURE 4: $Y_D^{\bullet}/Y_D$ difference spectra of unlabeled (a) and ring-4-^{13}C-Tyr-labeled (b) PS II core complexes of *Synechocystis* 6803. The sample was treated with NH_2OH to remove the Mn cluster followed by buffer washing. Sodium formate (100 mM) for preventing preoxidation of the non-heme iron and a ferricyanide/ferrocyanide (19 mM/1 mM) mixture as an exogenous electron acceptor were present in the sample. Flash illumination was performed by two successive pulses (1 s interval) from a Nd:YAG laser (532 nm, 7 ns). Sample temperature was 250 K.

to 1228 cm^{-1} upon labeling. This shifting band in the S_2/S_1 spectrum arises from an IR band of a tyrosine side chain, and thus the observation indicates that a tyrosine residue is present close to the Mn cluster and its vibrational mode is affected upon S_1-to-S_2 transition. It is noted that the band at 1251 cm^{-1} does not come from slightly contaminating acceptor-side signals; a Q_A^-/Q_A spectrum measured using the same *Synechocystis* core complexes was not affected by ring-4-^{13}C-Tyr labeling (data not shown) and an Fe^{2+}/Fe^{3+} spectrum originally does not have a negative band around 1250 cm^{-1} (*34*, *35*).

As a standard tyrosine spectrum in PS II, a $Y_D^{\bullet}/Y_D$ difference spectrum, which was recently obtained from the PS II membranes of spinach by Hienerwadel et al. (*32*), was measured using the *Synechocystis* core complexes and its isotopic effect was examined. Figure 4a shows a $Y_D^{\bullet}/Y_D$ spectrum obtained with the Mn-depleted core complexes of *Synechocystis* upon two-pulse illumination at 250 K. Because the efficiency of $Y_D^{\bullet}$ production upon one saturating flash is relatively low (*32*), only ∼60% of Y_D in the core sample was converted to $Y_D^{\bullet}$ upon 2 pulses judging from the intensity of a fully reacted $Y_D^{\bullet}/Y_D$ spectrum upon 20 pulses. The $Y_D^{\bullet}/Y_D$ spectrum in Figure 4a is virtually identical to the spectrum of spinach membranes (*32*), indicating that Y_D has the same structure and microenvironment between *Synechocystis* and higher plants. Upon ring-4-^{13}C-Tyr labeling (Figure 4b), a negative band at 1251 cm^{-1} and a positive band at 1502 cm^{-1} downshifted to 1226 and 1476 cm^{-1}, respectively, while other numerous bands remained basically unchanged. Hienerwadel et al. (*32*) previously assigned these bands at 1251 and 1502 cm^{-1} to the CO stretching modes of Y_D and $Y_D^{\bullet}$, respectively, by comparison with the IR spectra of cresol and its radical. The above frequency shifts upon ^{13}C labeling at the ring-4 position (^{13}C−O) (see Figure 1) support their assignments.

For further standards, FTIR spectra of tyrosine in aqueous solutions were measured at pH 0.6 (Tyr-OH) and pH 13.4 (Tyr-O$^-$). In Figure 5, the spectra of Tyr-OH (a) and Tyr-O$^-$ (b) are shown comparing unlabeled (thin line) and ring-4-^{13}C-labeled (thick line) tyrosine. In Tyr-OH, the relatively broad band at 1250 cm^{-1} downshifted to 1228 cm^{-1} upon isotopic labeling. IR and Raman studies of *p*-cresol (a model compound of tyrosine) have shown the CO stretching mode of phenolic hydroxyl group at ∼1255 cm^{-1} (*37*, *38*). The COH bending mode also appears in this frequency region; while in a non-hydrogen-bonding state it is located at ∼1180 cm^{-1} overlapping the CH bending band at ∼1170 cm^{-1}, its frequency increases up to the CO stretching frequency upon hydrogen bonding (*39*−*41*). Because *p*-cresol in aqueous solution shows CO stretching and COH bending bands at ∼1260 and ∼1240 cm^{-1}, respectively (*40*, *41*), the broad band of Tyr-OH at 1250 cm^{-1} (Figure 5a) is most likely ascribed to the overlap of the CO stretching and COH bending bands. Another strong band at 1519 cm^{-1} in the Tyr-OH spectrum, which is assignable to the ring CC stretching mode (*37*, *38*), downshifted to 1509 cm^{-1} upon ring-4-^{13}C labeling (Figure 5a). In the spectra of Tyr-O$^-$ (Figure 5b), on the other hand, the CO stretching band appeared at 1270 cm^{-1} and downshifted to 1246 cm^{-1} upon labeling. The ring CC mode of Tyr-O$^-$ was observed at 1499 cm^{-1}, which is 20 cm^{-1} lower than that of Tyr-OH, and showed a shift to 1490 cm^{-1}.

Effects of isotopic labeling on the S_2/S_1 and $Y_D^{\bullet}/Y_D$ spectra can be more clearly seen by taking double difference between

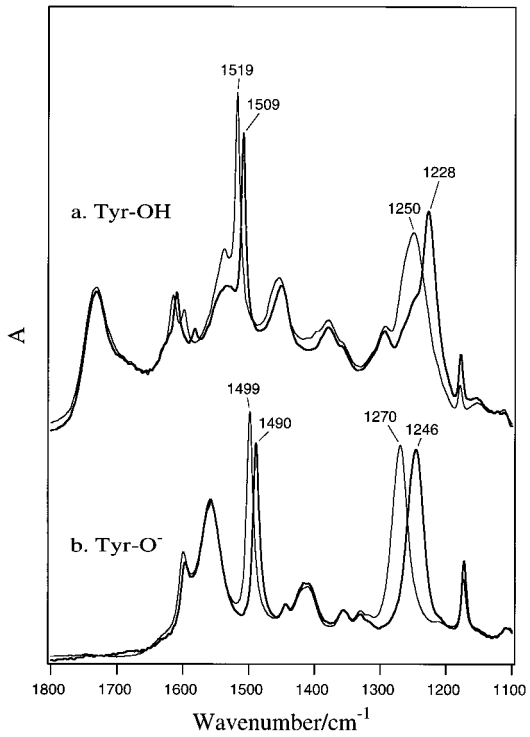

FIGURE 5: FTIR spectra of unlabeled L-tyrosine (thin line) and ring-4-^{13}C-labeled L-tyrosine (thick line) in aqueous solutions at pH 0.6 (Tyr-OH) (a) and at pH 13.4 (Tyr-O$^-$) (b). Tyrosine (2% w/v) was dissolved in 0.5 M HCl (for Tyr-OH) or 0.5 M NaOH (for Tyr-O$^-$) solution. The spectra of HCl and NaOH solutions were subtracted from the Tyr-OH and Tyr-O$^-$ spectra, respectively, so as to cancel the broad H_2O band around 1643 cm^{-1}. The spectra were measured at room temperature.

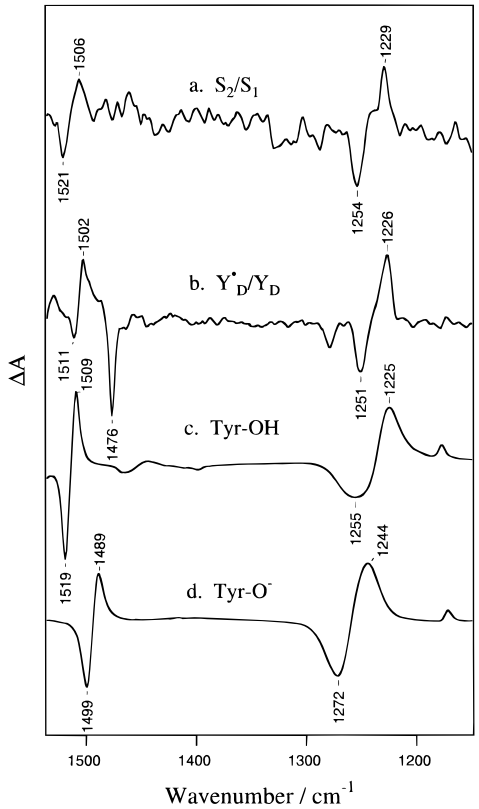

FIGURE 6: Effect of ring-4-^{13}C labeling of tyrosine on the spectra of S_2/S_1 (a), $Y_D^{\bullet}/Y_D$ (b), Tyr-OH (c), and Tyr-O$^-$ (d) as revealed by double difference (a, b) or difference (c, d) between the unlabeled and labeled spectra. The parent spectra for difference are in Figures 3, 4, 5a, and 5b for (a), (b), (c), and (d), respectively. For obtaining (a) and (b), the sign of the S_2/S_1 and $Y_D^{\bullet}/Y_D$ spectra was reversed before taking double difference so that the four spectra can be compared in the same phase.

unlabeled and labeled spectra. Figure 6 shows such double-difference spectra of S_2/S_1 (a) and $Y_D^{\bullet}/Y_D$ (b) compared with the difference spectra (labeled minus unlabeled) of Tyr-OH (c) and Tyr-O$^-$ (d). Note that because the neutral tyrosine bands in the S_2/S_1 and $Y_D^{\bullet}/Y_D$ spectra appeared in the negative sign, the sign of these spectra was reversed before taking double difference so that the four spectra can be compared in the same phase. Subtraction factors were determined so as to cancel unaffected bands in 1100−1530 cm^{-1} as much as possible. We did not show the spectral region higher than 1530 cm^{-1} in Figure 6, because the amide I (1600−1700 cm^{-1}) and amide II (∼1550 cm^{-1}) regions were highly sensitive to the sample condition, and hence subtle intensity changes were seen from sample to sample. However, in the region lower than 1530 cm^{-1}, the unshifted bands were well canceled by subtraction and only the bands affected by labeling remained (Figure 6).

In the CO region of tyrosine, the S_2/S_1 double-difference spectrum (Figure 6a) shows a simple differential signal with peaks at 1254 and 1229 cm^{-1} ($\Delta\nu = -25$ cm^{-1}), indicating that a negative band at 1254 cm^{-1} in the S_2/S_1 spectrum downshifts by 25 cm^{-1} upon ring-4-^{13}C-Tyr labeling. The peak frequencies of this differential signal are comparable to those of the 1251/1226 cm^{-1} signal ($\Delta\nu = -25$ cm^{-1}) in the $Y_D^{\bullet}/Y_D$ double-difference spectrum (Figure 6b) and of the 1255/1225 cm^{-1} signal ($\Delta\nu = -30$ cm^{-1}) in the Tyr-OH difference spectrum (Figure 6c). In contrast, the peak positions of the 1272/1244 cm^{-1} signal ($\Delta\nu = -28$ cm^{-1}) of the Tyr-O$^-$ spectrum (Figure 6d) are 15−18 cm^{-1} higher than the 1254/1229 cm^{-1} signal of S_2/S_1. In the $Y_D^{\bullet}/Y_D$ double-difference spectrum (Figure 6b), a signal at 1502/1476 cm^{-1} ($\Delta\nu = -26$ cm^{-1}), which is assignable to the CO stretching mode of $Y_D^{\bullet}$ (*32*), is observed. This feature is reasonably not observed in the other spectra that are not related to a tyrosine radical. Indeed, absence of this $Y_D^{\bullet}$ signal in the S_2/S_1 double-difference spectrum (Figure 6a) proves that there is no contamination of $Y_D^{\bullet}/Y_D$ signals in the S_2/S_1 difference spectrum.

In the ring CC region of tyrosine, a differential signal with peaks at 1521/1506 cm^{-1} ($\Delta\nu = -15$ cm^{-1}) appears in the S_2/S_1 double-difference spectrum (Figure 6a). This band shift is not evident in the original S_2/S_1 spectra (Figure 3) due to the complex band feature in this region. The peak positions are close to the 1519/1509 cm^{-1} signal ($\Delta\nu = -10$ cm^{-1}) of Tyr-OH (Figure 6c) but 17−22 cm^{-1} higher than the 1499/1489 cm^{-1} signal ($\Delta\nu = -10$ cm^{-1}) of Tyr-O$^-$ (Figure 6d). The ring CC mode of Y_D could not be identified in the $Y_D^{\bullet}/Y_D$ double-difference spectrum (Figure 6b); some $Y_D^{\bullet}$ bands probably overlap in this region.

The above isotopic shifts of the S_2/S_1 bands upon ring-4-^{13}C-Tyr labeling and the comparison with those of the $Y_D^{\bullet}/Y_D$, Tyr-OH, and Tyr-O$^-$ spectra (Figure 6) provide the basic assignments of the 1254 and 1521 cm^{-1} bands in the S_2/S_1 spectrum to the CO and ring CC stretching modes of tyrosine. The close positions of these bands to the CO and CC bands of Tyr-OH and a large difference from those of Tyr-O$^-$ indicate that the tyrosine coupled to the Mn cluster is present in a protonated state. In this case, the COH bending mode is also expected to appear near the CO region. However,

we could not recognize such a band in the S_2/S_1 double-difference spectrum (Figure 6a), and thus the COH bending band may overlap the 1254 cm^{-1} peak. The definitive assignment of the COH mode needs further studies.

The tyrosine signals at both 1254/1229 and 1521/1506 cm^{-1} in the S_2/S_1 double-difference spectrum show a simple differential shape (Figure 6a). This indicates that these tyrosine modes appear in the S_2/S_1 spectrum as a simple negative band; that is, the original tyrosine bands reduce their intensities upon S_2 formation with little frequency change. If the frequency change had been the major effect upon S_2 formation, a tyrosine band would have shown a differential signal in the S_2/S_1 difference spectrum, and a more complex band shape with three or four peaks would have appeared in the double-difference spectrum.

DISCUSSION

Ring-4-^{13}C-Tyr labeling of PS II core complexes of *Synechocystis* showed the presence of the tyrosine bands, the CO stretching band (possibly including the COH bending band) at 1254 cm^{-1}, and the ring CC stretching band at 1521 cm^{-1} in the S_2/S_1 FTIR difference spectrum of OEC. These tyrosine bands appeared in the S_2/S_1 spectrum as a simple intensity decrease upon S_2 formation.

We have estimated the extent of intensity decrease of the 1254 cm^{-1} CO band by taking the intensity of the Y_D band at 1251 cm^{-1} (Figure 4a) as a standard in the PS II core sample. Scales of both the S_2/S_1 and $Y_D^{\bullet}/Y_D$ spectra were first normalized on the basis of the relative protein amount in the FTIR sample, which was estimated by the intensity of the amide I band ($\sim$1650 cm^{-1}) of the original spectra (before subtraction; not shown) after correction of the water contribution at $\sim$1640 cm^{-1}. Assuming that 60% of Y_D in the PS II sample reacted to give a $Y_D^{\bullet}/Y_D$ spectrum in Figure 4a while all of the OEC was converted to the S_2 state upon one saturating pulse, it was estimated that the tyrosine band at 1254 cm^{-1} lost $\sim$18% of its original intensity upon S_2 formation. On the other hand, rough simulation using Gaussian bands to match the band shape of the 1254/1229 cm^{-1} signal in Figure 6a showed that the frequency shift of the tyrosine CO band upon S_2 formation, if any, must be <1 cm^{-1}.

It has been generally accepted that one positive charge is accumulated on the Mn cluster upon S_2 formation on the basis of the upshift of K-edge energy of XANES spectrum (*42*) and the appearance of the multiline EPR signal in the S_2 state (*43*). Also, the S_2/S_1 FTIR spectrum with prominent features in the amide I and carboxylate stretching regions has been interpreted as indicating that relatively drastic changes in the polypeptide conformations and the carboxylate coordination occur in the OEC upon S_1-to-S_2 transition (*20, 21, 23*−*25*). Hence, two mechanisms are considered as possible causes for perturbation of the vibrational modes of a tyrosine near the Mn cluster upon S_2 formation. One is that the structural changes of the Mn cluster are transmitted to the tyrosine via direct linkage of chemical and/or hydrogen bonds. The other is the vibrational Stark effect, i.e., the mechanism that an electric field affects the frequencies and intensities of the IR bands (*44*−*49*). In fact, Breton et al. (*50*) have recently found that a differential signal centered around 1732 cm^{-1} in the Q_A^-/Q_A spectrum of the *Rhodobacter sphaeroides* reaction center arises from the 10a-ester C═O of bacteriopheophytin (H_A), which is located $\sim$10 Å away from Q_A. They have explained the appearance of this band as a slight frequency shift (2−4 cm^{-1}) by an electrostatic effect induced by Q_A^- generation.

The Stark tuning rates $\delta_{\nu E}$ (derivatives of harmonic frequencies with respect to the field strength) and the fractional IR cross-section changes δ_{SE} (derivatives of the logarithm of the line intensities with respect to the field strength) of some small molecules have been calculated at the *ab initio* level (*45*−*47*) and at the semiempirical level (*48*). The Stark effect on carbon monooxide (CO) has been most extensively studied, and its calculated values (*45*) have well agreed with the experimental ones (*44*). Although neither the experiment nor the calculation of the Stark effect on the CO mode of phenol or its derivatives has been reported so far, the calculated d_{nE} and d_{SE} values of CO [$\delta_{\nu E} = 5 \times 10^{-7}$ cm^{-1}/(V/cm); $\delta_{SE} = -5 \times 10^{-9}$ cm/V] (*45*) are similar to the values of the CO stretching modes of H_2CO [$\delta_{\nu E} = 5.6 \times 10^{-7}$ cm^{-1}/(V/cm); $\delta_{SE} = -1.07 \times 10^{-9}$ cm/V] (*46*) and retinal [$\delta_{\nu E} = \sim 6 \times 10^{-7}$ cm^{-1}/(V/cm); $\delta_{SE} = \sim -1 \times 10^{-8}$ cm/V] (*48*). Andrés et al. (*46*) also have reported that the calculated d_{nE} and d_{SE} of various vibrational modes of H_2O, NH_3, H_2CO, and C_2H_4 fall in basically a similar range: $|\delta_{\nu E}| = 10^{-6}-10^{-8}$ cm^{-1}/(V/cm); $|\delta_{SE}| = 10^{-8}-10^{-10}$ cm/V. We therefore attempted to estimate the electrostatic effect on the tyrosine CO band using $\delta_{\nu E}$ and δ_{SE} of CO given by Andrés et al. (*45*). The band intensity was decreased by a factor of 0.82 upon S_2 formation (*vide supra*). Assuming only the electric field induced by Mn oxidation affects the IR band, the frequency shift that should accompany this intensity decrease was calculated to be 19.8 cm^{-1}. This estimated value clearly does not agree with the observation of little frequency shift (<1 cm^{-1}) upon S_2 formation. Thus, the change of the tyrosine band cannot be explained by a simple electrostatic effect. It is noted that although this estimation largely depends on the selection of $\delta_{\nu E}$ and δ_{SE}, the same conclusion is obtained from combination of rather wide ranges of $\delta_{\nu E}$ and δ_{SE} values.

The above consideration suggests that the coupling between the Mn cluster and the tyrosine via chemical and/or hydrogen bonds is the major cause for the change of the tyrosine bands. In this case, the tyrosine may directly interact with a ligand of the Mn cluster or it may be linked to the Mn cluster through a few amino acid residues.

The most probable candidate for the tyrosine coupled to the Mn cluster is Y_Z, which should be located close to the Mn cluster as an immediate electron donor. Two distinct views have been proposed from EPR about the distance between the Mn cluster and Y_Z, i.e., a very short one [4.5 Å (*9*)] and a relatively long one [$>$10Å (*15*) or 15-20 Å (*16*)]. As for another redox-active tyrosine Y_D, on the other hand, all of the groups that have studied the distance from the Mn cluster have basically agreed to the idea that the distance is much longer, i.e., 29−43 Å by Evelo et al. (*51*), 28−30 Å by Kodera et al. (*52*), and 25−35 Å by Un et al. (*53*). Also, the position of the CO band of the tyrosine in the S_2/S_1 spectrum and that of Y_D were different by 3 cm^{-1} for both unlabeled and labeled PS II (1254/1229 cm^{-1} in unlabeled/labeled S_2/S_1; 1251/1226 cm^{-1} in unlabeled/labeled Y_D) (Figure 6). The 3 cm^{-1} difference may have a real meaning under the relatively narrow band width ($\sim$14 cm^{-1}, hwfm), implying that the two signals originate from different species. Thus, Y_D as a candidate for the tyrosine residue coupled to the Mn cluster is less likely. The possibility of other redox-

inactive tyrosines for the candidate cannot be fully excluded; four such tyrosine residues are found on the lumenal side of the D1 polypeptide, in which the Mn cluster is most likely attached (*4*). All of them are located in the A−B loop or helix B, which might be involved in the Mn binding according to the PS II model by Svensson et al. (*54*). It is noted, however, that this model was obtained by adopting the relatively long distance (>10 Å) between Y_Z and the Mn cluster (*54*).

The major conclusion of this FTIR study, i.e., the presence of structural coupling between a tyrosine, most likely Y_Z, and the Mn cluster, is basically consistent with the recent proton or hydrogen atom abstraction model for the Y_Z function (*5*, *7*−*10*). The proposed direct abstraction may be possible, but if Y_Z is linked to the Mn cluster through a few amino acid residues by hydrogen bonds, this linkage will form a proton transfer pathway and an indirect proton transfer from substrate water to $Y_Z^{\bullet}$ will be realized. This proton or hydrogen atom transfer may occur in some of the S-state transitions such as S_3 to S_0. The chemical and/or hydrogen-bond connection between Y_Z and the Mn cluster also facilitates the electron transfer from the Mn cluster to $Y_Z^{\bullet}$ that takes place in every S-state transition. It is emphasized that the present FTIR study has detected the OEC−tyrosine coupling for the first time using an intact oxygen-evolving PS II sample.

REFERENCES

1. Diner, B. A., and Babcock, G. T. (1996) in O*xygenic Photosynthesis: The Light Reactions* (Ort, D. R., and Yocum, C. F., Eds.) pp 213−247, Kluwer, Dordrecht, The Netherlands.
2. Joliot, P., Barbieri, G., and Chabaud, R. (1969) *Photochem. Photobiol. 10*, 309−329.
3. Kok, B., Forbush, B., and McGloin, M. (1970) *Photochem. Photobiol. 11*, 457−475.
4. Debus, R. J. (1992) *Biochim. Biophys. Acta 1102*, 269−352.
5. Britt, R. D. (1996) in *Oxygenic Photosynthesis: The Light Reactions* (Ort, D. R., and Yocum, C. F., Eds.) pp 137−164, Kluwer, Dordrecht, The Netherlands.
6. Yachandra, V. K., DeRose, V. J., Latimer, M. J., Mukerji, I., Sauer, K., and Klein, M. P. (1993) *Science 260*, 675−679.
7. Hoganson, C. W., Lydakis-Simantiris, N., Tang, X.-S., Tommos, C., Warncke, K., Babcock, G. T., Diner, B. A., McCracken, J., and Styring, S. (1995) *Photosynth. Res. 46*, 177−184.
8. Tommos, C., Tang, X.-S., Warncke, K., Hoganson, C. W., Styring, S., McCracken, J., Diner, B. A., and Babcock, G. T. (1995) *J. Am. Chem. Soc. 117*, 10325−10335.
9. Gilchrist, M. L., Ball, J. A., Randall, D. W., and Britt, R. D. (1995) *Proc. Natl. Acad. Sci. U.S.A. 92*, 9545−9549.
10. Tang, X.-S., Randall, D. W., Force, D. A., Diner, B. A., and Britt, R. D. (1996) *J. Am. Chem. Soc. 118*, 7638−7639.
11. Mino, H., and Kawamori, A. (1994) *Biochim. Biophys. Acta 1185*, 213−220.
12. Force, D. A., Randall, D. W., Britt, R. D., Tang, X.-S., and Diner, B. A. (1995) *J. Am. Chem. Soc. 117*, 12643−12644.
13. Tang, X.-S., Zheng, M., Chisholm, D. A., Dismukes, G. C., and Diner, B. A. (1996) *Biochemistry 35*, 1475−1484.
14. Un, S., Tang, X.-S., and Diner, B. A. (1996) *Biochemistry 35*, 679−684.
15. Hoganson, C. W., and Babcock, G. T. (1988) *Biochemistry 27*, 5848−5855.
16. Kodera, Y., Hara, H., Astashkin, A. V., Kawamori, A., and Ono, T. (1995) *Biochim. Biophys. Acta 1232*, 43−51.
17. Astashkin, A. V., Mino, H., Kawamori, A., and Ono, T. (1997) *Chem. Phys. Lett. 272*, 506−516.
18. Mäntele, W. (1995) in *Anoxygenic Photosynthetic Bacteria* (Blankenship, R. E., Madigan, M. T., and Bauer, C. E., Eds.) pp 627−647, Kluwer, Dordrecht, The Netherlands.
19. Nabedryk, E. (1996) in *Infrared Spectroscopy of Biomolecules* (Mantsch, H. H., and Chapman, D., Eds.) pp 39−81, Wiley-Liss, New York.
20. Noguchi, T., Ono, T., and Inoue, Y. (1992) *Biochemistry 31*, 5953−5956.
21. Noguchi, T., Ono, T., and Inoue, Y. (1992) in *Research in Photosynthesis* (Murata, N., Ed.) Vol. II, pp 309−312, Kluwer, Dordrecht, The Netherlands.
22. Noguchi, T., Ono, T., and Inoue, Y. (1993) *Biochim. Biophys. Acta 1143*, 333−336.
23. Noguchi, T., Ono, T., and Inoue, Y. (1995) *Biochim. Biophys. Acta 1228*, 189−200.
24. Noguchi, T., Ono, T., and Inoue, Y. (1995) *Biochim. Biophys. Acta 1232*, 59−66.
25. Noguchi, T., Ono, T., and Inoue, Y. (1995) in *Photosynthesis: from Light to Biosphere* (Mathis, P., Ed.) Vol. II, pp 235−240, Kluwer, Dordrecht, The Netherlands.
26. Rippka, R., Deruelles, J., Waterbury, J. B., Herdman, M., and Stanier, R. Y. (1979) *J. Gen. Microbiol. 111*, 1−61.
27. Barry, B. A., and Babcock, G. T. (1987) *Proc. Natl. Acad. Sci. U.S.A. 84*, 7099−7103.
28. Tang, X.-S., and Diner, B. A. (1994) *Biochemistry 33*, 4595−4603.
29. Berthold, D. A., Babcock, G. T., and Yocum, C. F. (1981) *FEBS Lett. 134*, 231−234.
30. Ono, T., and Inoue, Y. (1986) *Biochim. Biophys. Acta 850*, 380−389.
31. Zimmermann, J.-L., and Rutherford, A. W. (1986) *Biochim. Biophys. Acta 851*, 416−423.
32. Hienerwadel, R., Boussac, A., Breton, J., and Berthomieu, C. (1996) *Biochemistry 35*, 15447−15460.
33. Berthomieu, C., Nabedryk, E., Mäntele, W., and Breton, J. (1990) *FEBS Lett. 269*, 363−367.
34. Hienerwadel, R., and Berthomieu, C. (1995) *Biochemistry 34*, 16288−16297.
35. Noguchi, T., and Inoue, Y. (1995) *J. Biochem. 118*, 9−12.
36. Steenhuis, J. J., and Barry, B. A. (1996) *J. Am. Chem. Soc. 118*, 11927−11932.
37. Jakobsen, R. J. (1965) *Spectrochim. Acta 21*, 433−442.
38. Takeuchi, H., Watanabe, N., and Harada, I. (1988) *Spectrochim. Acta 44A*, 749−761.
39. Hall, A., and Wood, J. L. (1967) *Spectrochim. Acta 23A*, 2657−2667.
40. Takeuchi, H., Watanabe, N., Satoh, Y., and Harada, I. (1989) *J. Raman Spectrosc. 20*, 233−237.
41. Gerothanassis, I. P., Birlirekis, N., Sakarellos, C., and Marraud, M. (1992) *J. Am. Chem. Soc. 114*, 9043−9047.
42. Yachandra, V. K., Guiles, R. D., McDermott, A. E., Cole, J. L., Britt, R. D., Dexheimer, S. L., Sauer, K., and Klein, M. P. (1987) *Biochemistry 26*, 5974−5981.
43. Dismukes, G. C., and Siderer, Y. (1981) *Proc. Natl. Acad. Sci. U.S.A. 78*, 274−278.
44. Lambert, D. K. (1988) *J. Chem. Phys. 89*, 3847−3860.
45. Andrés, J. L., Duran, M., Lledós, A., and Bertrán, J. (1991) *Chem. Phys. 151*, 37-43.
46. Andrés, J. L., Martí, J., Duran, M., Lledós, A., and Bertrán, J. (1991) *J. Chem. Phys. 95*, 3521−3527.
47. Andrés, J. L., Bertrán, J., Duran, M., and Martí, J. (1994) *J. Phys. Chem. 98*, 2803−2808.
48. Martí, J., Lledós, A., Bertrán, J., and Duran, M. (1992) *J. Comput. Chem. 13*, 821−829.
49. Bishop, D. M. (1993) *J. Chem. Phys. 98*, 3179−3184.
50. Breton, J., Nabedryk, E., Allen, J. P., and Williams, J. C. (1997) *Biochemistry 36*, 4515−4525.
51. Evelo, R. G., Styring, S., Rutherford, A. W., and Hoff, A. J. (1989) *Biochim. Bioiphys. Acta 973*, 428−442.
52. Kodera, Y., Dzuba, S. A., Hara, H., and Kawamori, A. (1994) *Biochim. Biophys. Acta 1186*, 91−99.
53. Un, S., Brunel, L.-C., Brill, T. M., Zimmermann, J.-L., and Rutherford, A. W. (1994) *Proc. Natl. Acad. Sci. U. S. A. 91*, 5262−5266.
54. Svensson, B., Vass, I., Cedergren, E., and Styring, S (1990) *EMBO J. 9*, 2051−2059.

BI971760Y